Wet-Chemical Analysis of Surface Concentration of Accessible Groups on Different Amino-Functionalized Mesoporous SBA-15 Silicas

Jessica M. Rosenholm and Mika Lindén*

Department of Physical Chemistry, Åbo Akademi University, Porthansgatan 3-5, FIN-20500 Turku, Finland

Received May 12, 2007. Revised Manuscript Received July 3, 2007

Surface functionalization is one of the key steps toward the utilization of mesoporous materials in different applications. In this study, we characterized amino-functionalized mesoporous SBA-15 silicas that have been prepared by different means; co-condensation, post-grafting of amino-silanes, and surface hyperbranching polymerization of poly(ethylene imine). Special focus is put on the accessibility of the introduced function. The materials are thoroughly characterized both by structural and by surface chemical means. We generally observe a good agreement between the *C*-value derived from BET surface area analysis, the number of accessible amine groups determined by quantitative imine reaction in solution, and zeta-potential measurements. Furthermore, indirect information about differences in the number of amine groups present on the outside surface of the particles can also be obtained. Our results clearly show that there are large differences between the availability of the amine function for materials functionalized by different methods and that the differences calculated as the number of accessible amine groups per unit area can be as large as 20-fold. The co-condensation route is the least efficient surface functionalization method under the studied conditions, and we actually observed a decrease not only in the relative but also the absolute number of accessible amine groups per unit area with an increasing amino-silane molar fraction for the co-condensed materials, which indicates that the commonly used gravimetrical means for determining the extent of true surface functionalization may give rise to large errors. Surface polymerization leads to the highest number of accessible amine groups, but often, the first polymerization cycle leads to polymer formation in micropores in the mesopore walls, which renders these amine groups inaccessible. These results demonstrate that the real surface composition of surface-functionalized mesoporous materials may have very little in common with the schematic representations often found in the literature.

Introduction

Mesoporous and mesoscopically ordered silicas followed by a wide variety of other metal oxides have attracted vast scientific and technological attention after the first full reports of the synthesis and characterization of this interesting class of materials appeared in the early 1990s.[1,2] This is due to their unique properties, which include a narrow pore size distribution, a high specific surface area and pore volume, and tunable pore sizes and structures,[3] making this class of materials interesting for application in the fields of catalysis, chromatography, sensing, size-selective separation, controlled immobilization or release of biologically active molecules, and nanoreactors.[4,5] Importantly, interfacial chemistry can readily be altered by methods developed for regular silica, including surface grafting of functional silanes, polymer coating, covalent linking of complexes, and co-condensation.[4,6] Hence, successful surface modification is often an integrated and crucial part of the material processing and is the basis for the functionality of the material. These functional groups provide further accessibility for anchoring other substrates (or complexes), such as biomolecules or metal ions, into the pore channels of the carrier material.

Two commonly applied methods for the introduction of functional groups onto the silica surface, in addition to the surface silanols, are co-condensation and post-grafting of functional silanes. Certain drawbacks are associated with both methods. The post-synthesis grafting method typically results

(1) (a) Kresge, C. T.; Leonowicz, M. E.; Roth, W. J.; Vartuli, J. C. *Nature* **1992**, *359*, 710. (b) Beck, J. S.; Vartuli, J. C.; Roth, W. J.; Leonowicz, M. E.; Kresge, C. T.; Schmitt, K. D.; Chu, C. T. W.; Olson, D. H.; Sheppard, E. W.; McCullen, S. B.; Higgins, J. B.; Schenker, J. L. *J. Am. Chem. Soc.* **1992**, *114*, 10834.

(2) Yanagisawa, T.; Shimizu, T.; Kuroda, K.; Kato, C. *Bull. Chem. Soc. Jpn.* **1990**, *63*, 988.

(3) (a) Taguchi, A.; Schüth, F. *Microporous Mesoporous Mater.* **2005**, *77*, 1. (b) Fajula, F.; Galarneau, A.; Di Renzo, F. *Microporous Mesoporous Mater.* **2005**, *82*, 227. (c) Lindén, M.; Schacht, S.; Schüth, F.; Steel, A.; Unger, K. *J. Porous. Mater.* **1998**, *5*, 177. (d) Ciesla, U.; Schüth, F. *Microporous Mesoporous Mater.* **1999**, *27*, 131. (e) Tuel, A. *Microporous Mesoporous Mater.* **1999**, *27*, 151. (f) Liu, Y.; Pinnavaia, T. J. *J. Mater. Chem.* **2002**, *12*, 3179. (g) Soler-Illia, G. J. de A. A.; Sanchez, C.; Patarin, J. *Chem. Rev.* **2002**, *102*, 4093. (h) Schüth, F. *Chem. Mater.* **2001**, *13*, 3184.

(4) Fryxell, G. E.; Liu, J. In *Adsorption on Silica Surfaces*; Papirer, E., Ed.; Marcel Dekker, Inc.: New York, 2000; pp 665−687 and references therein.

(5) Cao, G. *Nanostructures and Nanomaterials. Synthesis, Properties, and Applications*; Imperial College Press: London, 2004.

(6) (a) Wight, A. P.; Davis, M. E. *Chem. Rev.* **2002**, *102*, 3589. (b) Ford, D. M.; Simanek, E. E.; Shantz, D. F. *Nanotechnology* **2005**, *16*, 458. (c) Lim, M. H.; Stein, A. *Chem. Mater.* **1999**, *11*, 3285. (d) Yoshitake, H. *New J. Chem.* **2005**, *29*, 1107. (e) Fryxell, G. E. *Inorg. Chem. Commun.* **2006**, *9*, 1141.

10.1021/cm071289n CCC: $37.00
Published on Web 09/07/2007

in inhomogeneous surface coverage due to organic moieties congregating near the entries of the mesopores and the exterior surfaces.[7] The low reactivity of the surface silanols themselves or incomplete surface coverage due to, for example, limited reactivity of surface silanols may also limit the extent of surface functionalization by post-grafting.[8] The solvent used plays a crucial role, and whereas the silanization is most often conducted in organic solvents, the role of the trace water physisorbed on the silica surface is also of utmost importance.[9−11] Under water-free conditions, the concentration and distribution of organic moieties by the post-grafting method is constrained by the number of surface silanol groups and by their accessibility.[7] The extent of surface functionalization is often studied by thermogravimetry, but quantification of thermogravimetric data is not straightforward, unless additional detailed ^{13}C and ^{29}Si NMR studies are performed to quantitatively determine the degree of silane condensation as well as the extent of silane hydrolysis. Direct synthesis of surface-functionalized mesoporous silica by co-condensation, first reported in 1996 by Mann and co-workers,[12] has been reported to enable a higher and more homogeneous distribution of organosilane functionalities[13,14] but generally at the expense of mesoscopic ordering. Furthermore, co-condensation may also lead to situations where some of the functional groups are embedded in the silica network. This may be a serious drawback, as in applications of functionalized mesoporous silica, the effective surface concentration of functional groups is crucial.

In a recent study, we investigated the surface concentration of accessible carboxylic acid groups in mesoporous siliceous SBA-15 materials by benzylamine adsorption from solution, where the carboxylic acid functions were introduced either by a co-condensation approach or by surface polymerization of poly(methacrylic acid).[15] In both cases, only about 40% of the accessible surface groups on the surface-functionalized materials was carboxylic acid functions, while about 60% of the surface groups was silanols. Furthermore, about 1/5 of the surface silanols on SBA-15 was single (Q^3) silanols and 4/5 geminal (Q^2) silanols, where the respective pK_a values were about 2 and 8.2. These results demonstrate that the real surface composition of surface-functionalized mesoporous materials may have very little in common with the schematic representations often found in the literature.

In the present study, we extend our investigations to amino-functionalized mesoporous SBA-15. Aminopropyl-functionalized mesoporous silica has been found to be useful for some base-catalyzed reactions, wastewater treatment, further post-synthesis functionalization, and as heavy metal and toxic oxyanion sorbents,[16−25,30−31] to name a few. Furthermore, amino-functionalized mesoporous hosts have recently attracted much attention, especially regarding the immobilization of enzymes[26,27] or other proteins.[28] In addition to the conventional co-condensation and post-grafting approaches, other means of surface functionalization of silica by amino groups include multistep functionalization by attachment of different polyamines[29] or dendrimers[30,31] to pre-grafted mesoporous substrates and surface growth of hyperbranched polyethyleneimine (PEI).[32] Other sophisticated approaches used have included a stepped templated sol−gel technology,[33] molecular patterning techniques,[34] the use of benzyl spacers,[35] as well as the use of imprinted bulk silicas[36,37] and protected amino groups[38] when well-defined surfaces with site-isolated groups have been desired. There are also other attempts of ways of improving the effective amino group content via the co-condensation method, such as using di- or tri-amino-organoalkoxysilanes[21] or employing co-condensation via the anionic structure directing agent

(7) Lim, M. H.; Stein, A. *Chem. Mater.* **1999**, *11*, 3285.
(8) Kim, O. K.; Cho, S. J.; Park, J. W. *J. Colloid Interface Sci.* **2003**, *260*, 374.
(9) Wassermann, S. R.; Tao, Y.-T.; Whitesides, G. M. *Langmuir* **1989**, *5*, 1074.
(10) Silberzan, P.; Léger, L.; Ausseré, D.; Benattar, J. J. *Langmuir* **1991**, *7*, 1647.
(11) (a) Feng, X.; Fryxell, G. E.; Wang, L. Q.; Kim, A. Y.; Liu, J.; Kemner, K. M. *Science* **1997**, *276*, 923. (b) Liu, J.; Feng, X. D.; Fryxell, G. E.; Wang, L. Q.; Kim, A. Y.; Gong, M. L. *Adv. Mater.* **1998**, *10*, 161.
(12) Burkett, S. L.; Sims, S. D.; Mann, S. *Chem. Commun.* **1996**, 1367.
(13) Walcarius, A.; Delacote, C. *Chem. Mater.* **2003**, *15*, 4181.
(14) Richer, R.; Mercier, L. *Chem. Commun.* **1998**, 1775.
(15) Rosenholm, J. M.; Czuryszkiewicz, T.; Kleitz, F.; Rosenholm, J. B.; Lindén, M. *Langmuir* **2007**, *23*, 4315.
(16) Fryxell, G. E.; Liu, J.; Hauser, T. A.; Nie, Z.; Ferris, K. F.; Mattigod, S.; Gong, M.; Hallen, R. T. *Chem. Mater.* **1999**, *11*, 2148.
(17) Wang, X.; Lin, K. S. K.; Chan, J. C. C.; Cheng, S. *J. Phys. Chem. B* **2005**, *109*, 1763.
(18) Wang, X.; Lin, K. S. K.; Chan, J. C. C.; Cheng, S. *Chem. Commun.* **2004**, 2762.
(19) Yokoi, T.; Yoshitake, H.; Yamada, T.; Kubota, Y.; Tatsumi, T. *J. Mater. Chem.* **2006**, *16*, 1125.
(20) (a) Yoshitake, H.; Yokoi, T.; Tatsumi, T. *Chem. Mater.* **2002**, *14*, 4603. (b) Yoshitake, H.; Yokoi, T.; Tatsumi, T. *Bull. Chem. Soc. Jpn.* **2003**, *76*, 847. (c) Yokoi, T.; Tasumi, T.; Yoshitake, H. *Stud. Surf. Sci. Catal.* **2003**, *146*, 531. (d) Yokoi, T.; Tatsumi, T.; Yoshitake, H. *J. Colloid Interface Sci.* **2004**, *274*, 451.
(21) Yoshitake, H.; Yokoi, T.; Tatsumi, T. *J. Mater. Chem.* **2004**, *14*, 951.
(22) (a) Macquarrie, D. J.; Jackson, D. B. *Chem. Commun.* **1997**, 1781. (b) Utting, K. A.; Macquarrie, D. J. *New J. Chem.* **2000**, *24*, 591.
(23) (a) Cauvel, A.; Renard, G.; Brunel, D. *J. Org. Chem.* **1997**, *62*, 749. (b) Lasperas, M.; Llorett, T.; Chaves, L.; Rodrigues, I.; Cauvel, A.; Brunel, D. *Stud. Surf. Sci. Catal.* **1997**, *108*, 75. (c) Brunel, D. *Microporous Mesoporous Mater.* **1999**, *27*, 329. (d) Brunel, D.; Fajula, F.; Nagy, J. B.; Deroide, B.; Verhoef, M. J.; Veum, L.; Peters, J. A.; van Bekkun, H. *Appl. Catal., A* **2001**, *213*, 73.
(24) Bois, L.; Bonhommé, A.; Ribes, A.; Bernadette, P.; Raffin, G.; Tessier, F. *Colloids Surf., A* **2003**, *221*, 221.
(25) Brunel, D. *Microporous Mesoporous Mater.* **1999**, *27*, 329.
(26) (a) Maria Chong, A. S.; Zhao, X. S. *J. Phys. Chem. B* **2003**, *107*, 12650. (b) Maria Chong, A. S.; Zhao, X. S. *Appl. Surf. Sci.* **2004**, *237*, 398. (c) Maria Chong, A. S.; Zhao, X. S. *Catal. Today* **2004**, *93−95*, 293. (d) Lei, C.; Shin, Y.; Liu, J.; Ackerman, E. J. *J. Am. Chem. Soc.* **2002**, *124*, 11242. (e) Yiu, H. H. P.; Wright, P. A.; Botting, N. P. *J. Mol. Catal. B: Enzym.* **2001**, *15*, 81.
(27) Yiu, H. H. P.; Wright, P. A. *J. Mater. Chem.* **2005**, *15*, 3690.
(28) Han, Y.-J.; Stucky, G. D.; Butler, A. *J. Am. Chem. Soc.* **1999**, *121*, 9897.
(29) (a) Yoshitake, H.; Koiso, E.; Tatsumi, T.; Horie, H.; Yoshimura, H. *Chem. Lett.* **2004**, *33*, 872. (b) Yoshitake, H.; Koiso, E.; Horie, H.; Yoshimura, H. *Microporous Mesoporous Mater.* **2005**, *85*, 183.
(30) (a) Reynhardt, J. P. K.; Yang, Y.; Sayari, A.; Alper, H. *Chem. Mater.* **2003**, *16*, 4095. (b) Reynhardt, J. P. K.; Yang, Y.; Sayari, A.; Alper, H. *Adv. Funct. Mater.* **2005**, *15*, 1641. (c) Reynhardt, J. P. K.; Yang, Y.; Sayari, A.; Alper, H. *Adv. Synth. Catal.* **2005**, *347*, 1379.
(31) (a) Acosta, E. J.; Carr, C. S.; Simanek, E. E.; Shantz, D. F. *Adv. Mater.* **2004**, *16*, 985. (b) Yoo, S.; Lunn, J. D.; Gonzalez, S.; Ristich, J. A.; Simanek, E. E.; Shantz, D. F. *Chem. Mater.* **2006**, *18*, 2935.
(32) Rosenholm, J. M.; Penninkangas, A.; Lindén, M. *Chem. Commun.* **2006**, 3909.
(33) Zhang, C.; Zhou, W.; Liu, S. X. *J. Phys. Chem. B* **2005**, *109*, 24319.
(34) McKittrick, M. W.; Jones, C. W. *Chem. Mater.* **2003**, *15*, 1132.
(35) Hicks, J. C.; Jones, C. W. *Langmuir* **2006**, *22*, 2676.
(36) (a) Defreese, J. L.; Katz, A. *Microporous Mesoporous Mater.* **2006**, *89*, 25. (b) Bass, J. D.; Katz, A. *Chem. Mater.* **2003**, *15*, 2757.
(37) Bass, D.; Katz, A. *Chem. Mater.* **2006**, *18*, 1161.
(38) Mehdi, A.; Reyé, C.; Brandès, S.; Guilard, R.; Corriu, R. J. P. *New J. Chem.* **2005**, *29*, 965.

route.[19,39−41] Recently, we were successfully able to produce reactive primary amine groups on the surface of mesoporous SBA-15 in the form of a surface-grown PEI by an acid-catalyzed hyperbranching polymerization approach,[32] a method that previously had been used for the functionalization of fused silica, silicon wafers, and glass.[8] An advantage is that the method is very straightforward and actually conducted in the same manner as simple post-synthesis grafting (in contrast to complex multistep functionalization, where generally a pre-functionalization is needed). PEI is the cationic polymer exhibiting the highest positive charge density when fully protonated in aqueous solution.[42] Utilizing the high quantity of primary amino groups providing a high positive charge density, PEI has been successfully used as, for instance, a polymer film on cell adhesion substrates (instead of poly-L-LYSINE),[43] as well as a versatile non-viral vector alternative for gene delivery.[44,45] Other application areas for PEI include the paper industry as well as wastewater treatments, where its chelating properties are used to remove metal ions.[46] The monomer aziridine is highly reactive and very small, making it a promising candidate for successful polymer functionalization of pores in the nanometer range.

The aim of the present study was to critically evaluate the surface chemistry of amino-functionalized mesoporous silica, with special focus on the effective concentration of accessible amine groups. The aim was not to evaluate all available means of amino functionalization and their variations but rather to establish experimental means of evaluating the surface concentration of accessible amine groups to achieve a better understanding for structure−activity relationships for surface-functionalized mesoporous materials. Three different means for amine surface functionalization were employed, co-condensation, post-grafting, and surface growth of PEI. Three different SBA-15 materials with different surface silanol concentrations were used as substrates for post-grafting and surface polymerization. Furthermore, three different amino-silanes were compared in the post-grafting. Amino-functionalized SBA-15 prepared according to the co-condensation approach was studied having the amino-silane content as the parameter. The efficiency of the different amino-functionalized SBA-15 materials to serve as substrates for surface growth of PEI was also studied. In addition to standard structural characterization, XRD, and N_2 sorption, the materials were characterized by thermogravimetry and zeta-potential measurements. Furthermore, we used the method described by Moon et al.[47] for quantification of the respective surface concentrations of accessible amine functions for the different materials. This method is based on reacting the surface primary amine groups with 4-nitrobenzaldehyde, followed by hydrolysis and determination of the amount of regenerated 4-nitrobenzaldehyde, and has recently been successfully employed for the determination of the effective surface concentration of primary amine groups in mesoporous amino-functionalized silica.[32] A similar imine formation reaction was used by Mehdi et al.,[38] where the excess benzaldehyde from the imine reaction was detected by gas chromatography. Our results clearly show that there are large differences between the availability of the amine function for materials functionalized by different methods and the differences calculated, as the number of accessible amine groups per unit area can be 20-fold. Furthermore, we also show that thermogravimety is not generally applicable as a single characterization method for the determination of the surface concentration of functional groups.

Experimental Procedures

Synthesis of SBA-15 Substrate Materials. Mesoporous silica SBA-15 parent materials were synthesized according to Choi et al.[48] using a triblock copolymer, Pluronic P123 ($EO_{20}PO_{70}EO_{20}$ BASF/Aldrich), as the structure directing agent. Tetraethoxysilane (TEOS 98% Aldrich) was used as the silica precursor with molar ratios of $n_{TEOS}/n_{P123} = 60$, and the synthesis mixture was aged for 24 h at 368 K prior to template removal. Template removal was conducted either via ethanol extraction prior to calcination, involving subsequent heating to 823 K with a 1 K/min heating ramp, or solely via solvent extraction by refluxing in sulfuric acid (48 wt %) at 368 K overnight. Rehydroxylation of calcined samples was performed by refluxing overnight in hydrochloric acid (18.5 wt %),[49] and rehydroxylated samples are referred to as RH in the following.

Synthesis of Amino-Silane Materials. *Co-condensation of Amino-SBA-15 with Varying Molar Ratios of 3-Aminopropyltriethoxysilane (APTS).*[17] Co-condensed amino-SBA-15 silicas with varying molar ratios were synthesized according to the procedure described by Wang et al.[17] using triblock-copolymer P123 (BASF) as the structure directing agent and APTS (ABCR) as the organosilane. The synthesis mixture had a composition of TEOS/APTS/HCl/P123/H_2O of $(1 - x):x$:6.1:0.017:165 and was stirred for 20 h at 308 K and subsequently aged at 363 K for 24 h. x was varied from 0 to 0.1, 0.15, and 0.2. The co-condensed materials were hence denoted CCX%, with X corresponding to the amount of APTS used in the synthesis. After filtration and drying, the material was extracted in 95% ethanol under reflux for 24 h as a suspension of 1.5 g of as-synthesized material per 400 mL of ethanol. For reference purposes, a similar material using only TEOS as the silica source was also prepared.

Post-synthesis Grafting. For the post-synthesis grafting, three different amino-silanes were used, 3-aminopropyltrimethoxysilane

(39) Yoshitake, H.; Yokoi, T.; Tatsumi, T. *Chem. Mater.* **2003**, *15*, 4536.
(40) Che, S.; Garcia-Bennett, A. E.; Yokoi, T.; Sakamoto, K.; Kunieda, H.; Terasaki, O.; Tatsumi, T. *Nat. Mater.* **2003**, 801.
(41) Yokoi, R.; Yoshitake, H.; Tatsumi, T. *Stud. Surf. Sci. Catal.* **2004**, *154*, 519.
(42) Ham, G. E. In *Polymeric Amines and Ammonium Salts*; Goethals, E. J., Ed.; Pergamon Press: Oxford, 1980.
(43) Lakard, S.; Herlem, G.; Propper, A.; Kastner, A.; Michel, G.; Vallès-Villarreal, N.; Gharbi, T.; Fahys, B. *Bioelectrochemistry* **2004**, *62*, 19.
(44) (a) Boussif, O.; Lezoualc'h, F.; Zantha, M. A.; Mergny, M. D.; Scherman, D.; Demeneix, B.; Behr, J.-P. *Proc. Natl. Acad. Sci. U.S.A.* **1995**, *92*, 7297. (b) Godbey, W. T.; Wu, K. K.; Mikos, A. G. *J. Controlled Release* **1999**, *60*, 149. (c) Godbey, W. T.; Wu, K. K.; Mikos, A. G. *Gene Ther.* **1999**, *6*, 1380. (d) Godbey, W. T.; Wu, K. K.; Mikos, A. G. *Proc. Natl. Acad. Sci. U.S.A.* **1999**, *96*, 5177.
(45) (a) von Harpe, A.; Petersen, H.; Li, Y.; Kissel, T. *J. Controlled Release* **2000**, *69*, 309. (b) Kunath, K.; von Harpe, A.; Fisher, D.; Petersen, H.; Bickel, U.; Voigt, K.; Kissel, T. *J. Controlled Release* **2003**, *89*, 113. (c) Kunath, K.; von Harpe, A.; Fischer, D.; Kissel, T. *J. Controlled Release* **2003**, *88*, 159.
(46) Matsumoto, K.; Suganuma, A.; Kunui, D. *Powder Technol.* **1980**, *25*, 1.
(47) Moon, J. H.; Shin, J. S.; Kim, S. Y.; Park, J. W. *Langmuir* **1996**, *12*, 4621.
(48) Choi, M.; Heo, W.; Kleitz, F.; Ryoo, R. *Chem. Commun.* **2003**, 1340.
(49) Kumar, D.; Schumacher, K.; du Fresne von Hohenesche, C.; Grün, M.; Unger, K. K. *Colloids Surf., A* **2001**, *187−188*, 109.

Table 1. Structural Data for Materials as Obtained from Nitrogen Sorption at 77 K and Powder XRD

material	A_s(BET) (m^2 g^{-1})	V_p (cm^3 g^{-1})	*C*-value	d_p (*nm*)	$V_\mu p$ (cm^3 g^{-1})	a_0 (*nm*)
		Substrates				
SBA-15	850	1.00	155	7.0	0.078	10.8
SBA-15 RH	513	0.90	154	8.5	0.033	10.6
SBA-15 Ex	*782*	*1.62*	*117*	*9.1*	*0.036*	*12.2*
		Co-condensed amino-silane				
CC10%-SBA-15	745	0.90	77	7.3	0.004	11.3
CC15%-SBA-15	663	0.71	88	6.6	0.022	11.4
CC20%-SBA-15	*660*	*0.65*	*131*	*6.6*	*0.044*	*11.5*
		Aminosilanized samples				
APS-SBA-15	493	0.64	64	6.3	0.006	
APTS-SBA-15	468	0.60	61	6.3	0.002	
APDEMS-SBA-15	604	0.76	78	6.3	0.007	
APTS-SBA-15 RH	314	0.57	54	7.0	0.000	
APTS-SBA-15 Ex	*442*	*1.07*	*47*	*8.2*	*0.000*	
		PEI-functionalized materials				
PEI-SBA-15	468	0.69	63	7.0	0.001	
PEI-SBA-152^{cyc} TOT	300	0.46	36	6.6	0.000	
PEI-SBA-15 RH	282	0.54	37	7.3	0.000	
PEI-SBA-15 Ex	389	0.89	32	8.8	0.000	
PEI-CC10%-SBA-15	176	0.29	35	6.1	0.000	
PEI-APTS-SBA-15	320	0.47	41	6.3	0.000	

(APS), APTS, and 3-(diethoxymethylsilyl)propylamine (APDEMS) (97%, Aldrich). As substrates, SBA-15 (SBA-15), solvent-extracted SBA-15 (SBA-15 Ex), and RH SBA-15 (SBA-15 RH) were used. The substrates were carefully vacuum-dried at a temperature of 373 K and sealed under vacuum to avoid the adsorption of excess water from the atmosphere and stored under nitrogen atmosphere prior to the addition of dry toluene. The silane was then added to the toluene under stirring in amounts corresponding to the approximate amount of surface silanol groups on the silica, which was calculated using a silanol surface excess value of 9 μmol m^{-2} for the extracted and RH samples and 4 μmol m^{-2} for the calcined materials. The silanization was carried out at 408 K under reflux and nitrogen atmosphere overnight. The same procedure was repeated for the calcined SBA-15 at room temperature for the three silanes. After the silanization reaction, the sample was filtered, washed with toluene, aged at 353 K for 3 h, and dried under vacuum at 318 K.

Polymerization Approaches. *Synthesis of Aziridine.* Aziridine was synthesized from aminoethylsulphuric acid (Aldrich) according to the procedure described by Allen et al.[50] Aminoethylsulphuric acid was mixed with a sodium hydroxide solution and heated in an oil bath. The bath was removed after boiling started and resumed as the mixture started to cool. About 100 mL of distillate boiling between 323 and 378 K was quickly collected. KOH was added to the cooled distillate, whereas the imine separated as an upper layer. The imine was then separated from the mixture and stored over KOH at 4 °C overnight. After observing that no aqueous layer appeared, the imine was decanted and distilled from KOH pellets yielding a clear colorless liquid boiling at 328−330 K.

Polymerization of Aziridine on the Material Surfaces. Similar to the post-grafting method, the surface polymerization of aziridine was performed with toluene as the solvent, in which the substrates were suspended after being carefully vacuum-dried and sealed under vacuum and subsequently subjected to an argon atmosphere. Catalytic amounts of acetic acid were added under stirring, after which aziridine was added in amounts enough for three generations to form on the respective substrates. The suspension was refluxed under argon atmosphere overnight at 348 K, filtered, washed with toluene, and dried in vacuo at 313 K. This procedure was conducted for SBA-15, SBA-15 Ex, SBA-15 RH, APTS-SBA-15, and CC10%-SBA-15. A second cycle (the previous procedure repeated twice) was carried out for calcined SBA-15.

Characterization Methods. *Powder XRD Measurements.* XRD measurements were performed using a Kratky compact small-angle system (M. Braun). The system was equipped with a position-sensitive detector (PSD 50 m) consisting of 1024 channels of 55.5 μm width each. A Seifert ID-300 X-ray generator, operating at a maximum intensity of 50 kV and 40 mA, provided the Cu Kα radiation at $\lambda = 1.542$ Å. A Ni filter was used to remove Kβ radiation, and a W filter protected the detector from the primary beam. The sample-to-detector distance was 277 mm. The sample holder was kept under vacuum during the measurements to minimize the background scattering from air.

Nitrogen Sorption at 77 K. Nitrogen physisorption measurements were performed at 77 K using an ASAP 2010 sorptometer (Micromeritics). The calcined SBA-15 materials were outgassed at 423 K prior to the measurements, while the functionalized materials were outgassed at 363 K. The NLDFT kernel (Autosorb 1 software, Quantachrome Instruments) developed for silica exhibiting a cylindrical pore geometry[51] was used for pores size and pore volume determination. For the substrate-based materials, the equilibrium model was used, while the adsorption branch model was used for the co-condensed materials.

Thermogravimetric Analysis. Thermogravimetic analyses were performed using a Netzsch TGA 209. Each sample was compared to a reference sample measured with the same background run and temperature program, which generally included heating up to 1173 K at a heating rate of 10 K/min under air. Nitrogen was used as a protective gas. The TGA runs were analyzed by the Netzsch Proteus Thermal Analysis Software, v. 4.3.1. The sample and reference were first normalized against the dry weight, then the reference was subtracted from the sample, and the mass loss was normalized to the mass of the substrate to yield the mass increase (in wt %) from the functionalization step in question.

Accessible Surface Amino Concentration Determined by Imine Functionalization and UV−vis Spectrophotometry. The total amount of accessible primary amino groups was determined by a surface-

(50) Allen, C. F. H.; Spangler, F. W.; Webster, E. R. In *Organic Synthesis*; Rabjohn, N., Ed.; Wiley: New York, 1963; Vol. IV, p 433.

(51) Ravikovitch, P. I.; Wei, D.; Chueh, W. T.; Haller, G. L.; Neimark, A. V. *J. Phys. Chem. B* **1997**, *101*, 3671.

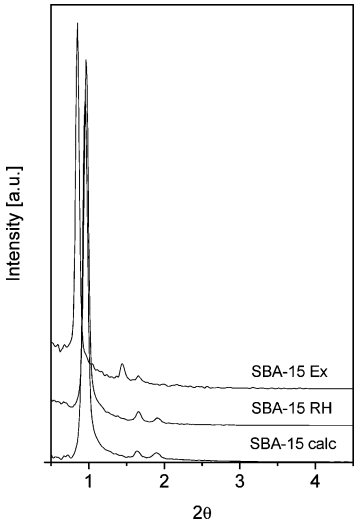

Figure 1. Powder X-ray diffraction patterns for the substrate materials.

imine formation procedure following the procedure of Moon et al.[47] with subsequent hydrolysis in aqueous solution. Again, the samples were carefully vacuum-dried at 343 K, sealed, and subjected to argon atmosphere. To this, a 4-nitrobenzaldehyde (anhydrous) methanolic solution (1 mg/mL) was added, with catalytic amounts of acetic acid. The suspension was stirred under reflux overnight at 323 K, filtered, washed with methanol, and dried in vacuo. Subsequently, the now imine-functionalized material was hydrolyzed in an acidic (acetic acid) aqueous solution of known volume at 313 K overnight. The regenerated imine concentration was determined spectrophotometrically (Shimadzu) at $\lambda = 269$ nm.

IEP Titrations. The IEP titrations were performed using a Malvern ZetaSizer NanoZS coupled to a MPT-2 titrator unit. The zeta-potential was measured as a function of pH by titrating with 0.5 M HCl and NaOH at 298 K. The samples were suspended in deionized water (1 mg/mL) and dispersed by sonication. Reverse titrations were performed to ensure chemical stability of the introduced surface function during the measurements.

Results and Discussion

Structural Characterization of Materials. Three different siliceous SBA-15 materials were used as support materials for the introduction of amine functions by post-synthesis methods. The structural characteristics of the synthesized materials are summarized in Table 1. For calcined SBA-15, three reflections were observed in XRD (Figure 1), and these could be indexed to *p*6*m* symmetry with a lattice spacing of 10.8 nm. The nitrogen sorption isotherm is shown in Figure 2 and is a type IV isotherm with parallel adsorption−desorption branches typical for this class of materials. The mesopore diameter is 7.0 nm, as determined by the equilibrium NLDFT method based on nitrogen sorption data at 77 K. The micropore volume was 0.078 cm^3/g, and the BET surface area was 850 m^2/g.

As the surface silanols are anchoring points for the amine functions introduced by post-synthesis approaches, we also used a RH procedure based on HCl treatment of the calcined material to increase the number of silanols. This method has previously been shown to lead to an increase in the surface silanol concentration from 2−4 to 5 μmol/m^2 for mesoporous

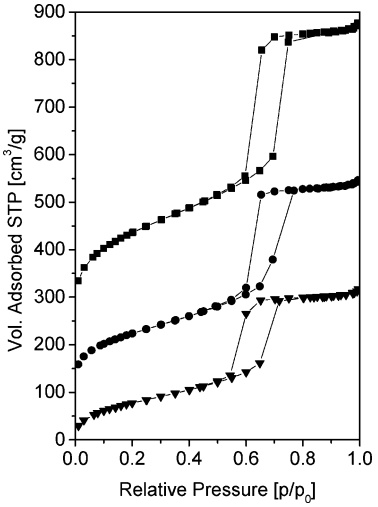

Figure 2. Nitrogen sorption isotherms measured at 77 K for calcined SBA-15 (■), offset by 200 $cm^3\ g^{-1}$; PEI-SBA-15 (●), offset by 100 $cm^3\ g^{-1}$; and PEI-SBA-15 2^{cyc}.

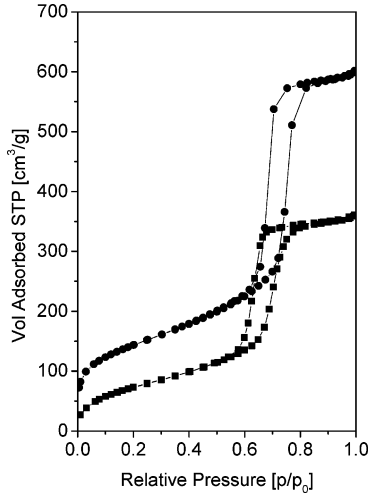

Figure 3. Nitrogen sorption isotherms measured at 77 K for RH SBA-15 RH (●) and PEI-SBA-15 RH (■).

MCM-41 materials.[49] These values can be compared to that of a fully hydroxylated silica surface, for which 8−9 μmol/m^2 has been suggested.[53] For MCM-41 materials, a loss of periodic structure was reported after RH, but the reason for this was suggested to be the thin mesopore walls. We did not observe any loss of order for the HCl-treated SBA-15 material, which clearly can be ascribed to the thicker pore walls of SBA-15. The lattice spacing of the calcined SBA-15 material remained virtually unaffected by HCl treatment, and also, in this case, three reflections that could be indexed to *p*6*m* symmetry were observed by XRD (Figure 1). The correspondning nitrogen sorption isotherm is shown in Figure 3, and it is evident that the capillary condensation step is shifted to higher relative pressures for the RH material, indicative of an increase in the pore diameter. The NLDFT equilibrium kernel gives a mesopore diameter of 8.5 nm. At the same time, the micropore volume and BET surface area decreased to 0.033 cm^3/g and 513 m^2/g, respectively. This indicates that the silica network became more condensed

(52) Choi, M.; Heo, W.; Kleitz, F.; Ryoo, R. *Chem. Commun.* **2003**, 1340.

(53) Zhuravlev, L. T. *Pure Appl. Chem.* **1989**, *61*, 1969.

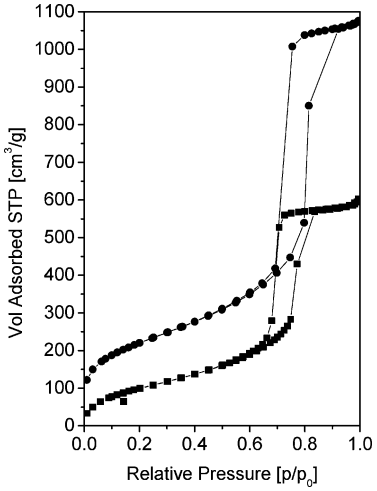

Figure 4. Nitrogen sorption isotherms measured at 77 K for extracted SBA-15 Ex (●) and PEI-SBA-15 Ex (■).

upon HCl treatment, which is also reflected in the slight decrease of the lattice parameter a_0 to 10.6 nm.

For SBA-15 materials, the surfactant removal step can also be performed by H_2SO_4 treatment instead of by thermal decomposition,[54] and here, H_2SO_4 will chemically decompose the portion of the surfactant that is located in the mesopores by ether cleavage but leave the portion of the surfactant that is located inside the silica network virtually unaffected.[54] This chemical method should also lead to a lower contraction of the unit cell upon surfactant removal as compared to calcination. This is in agreement with our findings since the lattice spacing increased to 12.2 nm and the mesopore diameter was 9.1 nm. The large mesopore diameter also gives this material a high mesopore volume, as is evident from the sorption isotherm shown in Figure 4. Furthermore, the micropore volume was 0.036 cm^3/g as compared to 0.078 cm^3/g for the calcined material. Four reflections that could be indexed to *p*6*m* symmetry were observed by XRD (Figure 1). The BET surface area was also relatively low, 782 m^2/g, again in agreement with the suggestion that the portion of the ethylene oxide chains that is buried in the silica walls remains much less affected by H_2SO_4 treatment as compared to the parts of the surfactants that are accessible in the mesopores.

The *C*-value in the BET analysis can be used to obtain information about the strength of the adsorbate−adsorbent interaction and is typically higher for more hydrophilic surfaces. For all three previously discussed siliceous materials, the *C*-values were in the range of 115−160, which are typical values for mesoporous silica.[55] However, we note that the presence of micropores can have a strong influence on the obtained *C*-values,[56] while these values should not be taken as an absolute measure. We also note that remaining organics in the form of EO chains in the micropores discussed previously might be read into the lower value of solvent-extracted SBA-15 as compared to both the other substrates.

We also used benzylamine adsorption from cyclohexane[15] onto the three different SBA-15 materials to determine the concentration of accessible surface silanols. The values were about 1, 1.2, and 1.6 mmol/g for the calcined, RH, and extracted SBA-15 materials. The corresponding values calculated per surface area were 1.2, 2.4, and 2.6 $\mu mol/m^2$, confirming that the concentration of surface silanols was higher for the RH and extracted materials as compared to the calcined material. The lower surface silanol concentrations for the SBA-15 materials as compared to MCM-41 materials can be understood, as the wall thickness of the SBA-15 materials is higher than that of MCM-41. For these MCM-41 materials,[49] the amount of silanols was determined either by thermogravimetry or by isotopic exchange with deuterated trifluoroacetic acid followed by ^1H NMR, which means that either the total amount of silanols is determined or for the latter probably both OH groups in each geminal surface silanol are seen. If this is the case, values up to 80% higher could be detected for surface silanols than, e.g., by benzylamine adsorption since in this case the benzylamine molecule is adsorbed only to one of the silanols belonging to a geminal silanol group.[15] In another study, the difference in the number of silanol groups between calcined and solvent-extracted MCM-41 has been determined by NMR,[57] and the silanol content was about 17% higher for the extracted sample as compared to the calcined sample, 3.0 nm^{-2} for the extracted and 2.5 nm^{-2} for the calcined material. However, the maximum concentration of the attached chlorotrimethylsilane (TRMS) was 0.75 nm^{-2} (corresponding to a value of 1.25 $\mu mol/m^2$), and hence, 75% of the silanols were not accessible by surface silylation methods. This value is in good agreement with our results obtained by benzyl amine adsorption.

Co-condensed Materials. Co-condensed materials were synthesized using mixtures of TEOS and APTS according to the synthesis method of Wang et al.,[18] as this method was suggested to be superior to the conventional co-condensation methods at the time because of a prehydrolysis-step of TEOS before the addition of APTS. The APTS molar ratios were 10, 15, and 20% as related to the total silicon precursor content. XRD patterns are presented in Figure 5. The lattice spacings were slightly higher for the co-condensed materials as compared to the purely siliceous SBA-15 materials discussed previously, with lattice spacings of about 11.4 nm (see Table 1). The co-condensed samples were not as well-ordered as the purely siliceous SBA-15 materials, in agreement with previous reports,[21] and the long-range order decreased with increasing APTS content, as judged from the gradually decreasing intensity of the higher order reflections in XRD, while the lattice spacing did not change dramatically. The nitrogen sorption isotherms of the co-condensed materials are shown in Figure 6. The width of the adsorption−desorption hysteresis increased with an increasing APTS content, and the wide hysteresis observed especially

(54) Yang, C.-M.; Zibrovius, B.; Schmidt, W.; Schüth, F. *Chem. Mater.* **2004**, *16*, 2918.
(55) Rouquerol, F.; Rouquerol, J.; Sing, K. *Adsorption by Powders and Solids: Principles, Methodology, and Applications*; Academic Press: London, 1999.
(56) (a) De Witte, B.; Vercruysse, K.; Aernouts, K.; Verwimp, P.; Uytterhoeven, J. B. *J. Porous Mater.* **1996**, *2*, 307. (b) Basaldella, E. I.; Tara, J. C.; Aguilar Armenta, G.; Patiño-Iglesias, M. E.; Rodríguez Castellón, E. *J. Sol.-Gel Sci. Technol.* **2006**, *37*, 141.
(57) Zhao, X. S.; Lu, G. Q.; Whittaker, A. K.; Millar, G. J.; Zhu, H. Y. *J. Phys. Chem. B* **1997**, *101*, 6525.

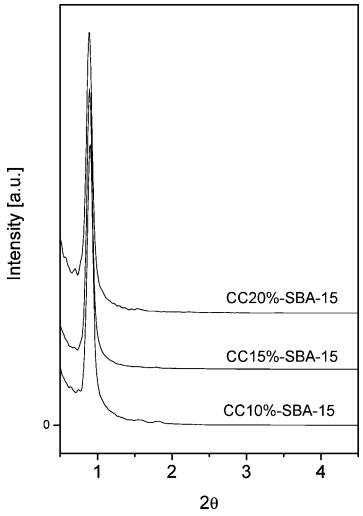

Figure 5. Powder X-ray diffraction patterns for the co-condensed materials with different amounts of APTS.

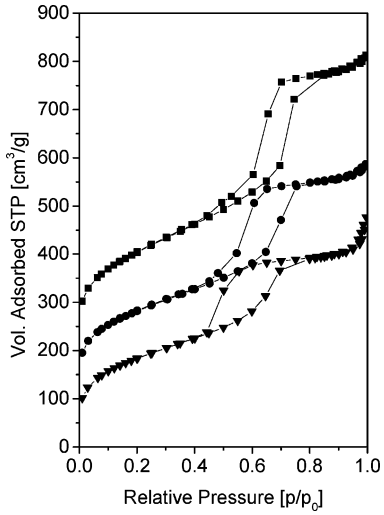

Figure 6. Nitrogen sorption isotherms measured at 77 K for CC10%-SBA-15 (■), offset by 200 cm^3 g^{-1}; CC15%-SBA-15 (●), offset by 100 cm^3 g^{-1}; and CC20%-SBA-15.

for the CC20% material was not compatible with a pore system consisting of straight cylinders but rather indicates the presence of pores with a strongly corrugated cylindrical geometry or spherical pores with smaller pore windows. In the latter case, the pore structure is not compatible with *p*6*m* symmetry but rather with cubic symmetry. The micropore volume is low for the CC10% material, 0.004 cm^3/g, and increases with an increasing APTS content, while the total pore volume decreases. The *C*-values are lower for the co-condensed materials as compared to the purely siliceous materials, which could be expected due to the presence of a more hydrophobic surface function in these materials. However, interestingly, the lowest value, 77, is observed for the CC10% material, while the corresponding value for the CC20% material, 131, is fairly close to that obtained for the purely siliceous materials. Thus, we note at this stage that the nitrogen sorption results indicate that the highest surface concentration of amino groups for the co-condensed materials is obtained for fairly low total APTS contents. We will return to this discussion in more detail next.

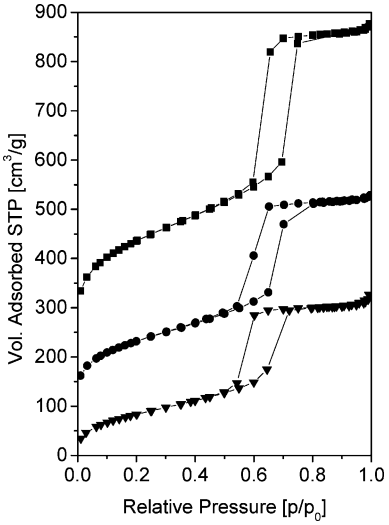

Figure 7. Nitrogen sorption isotherms measured at 77 K for calcined SBA-15 (■), offset by 200 cm^3 g^{-1}; APTS-SBA-15 (●), offset by 100 cm^3 g^{-1}; and PEI-APTS-SBA-15.

Post-functionalized Materials. The SBA-15 materials discussed previously were functionalized with amino-silanes in toluene, which is a commonly used procedure. The nitrogen sorption isotherms for materials functionalized with APTS are shown in Figure 7, and the derived parameters are summarized in Table 1. A significant reduction in specific surface area, total pore volume, and mesopore volume was observed, as can be expected for a successful grafting. Furthermore, the pore diameter decreased by about 1 nm upon grafting, but the lattice parameter remained unchanged. Strikingly, the microporosity was almost absent for all grafted materials. The *C*-values were generally low, 47−64, but clear differences between the different SBA-15 starting materials were observed. The amino-silane grafting was very reproducible, and no significant differences between APS- and APTS-functionalized materials were observed. The degree of surface functionalization was independent of the temperature within the temperature window studied. Some graftings were also performed using APDEMS, but the higher BET area, *C*-value, and mesopore volume observed suggest a less efficient surface functionalization for this silane.

PEI-Functionalized Materials. As the third means of surface functionalization, we used our recently published method for surface polymerization of aziridine to PEI on mesoporous silica[32] and used the siliceous SBA-15 materials as substrates. Furthermore, as it was reported that direct polymerization of PEI from flat silica substrates is slightly less effective in terms of hyperbranching as compared to the corresponding aminosilylated surfaces,[8] two distinctly different aminopropyl-functionalized substrates were PEI functionalized, namely, CC10%-SBA-15 and APTS-SBA-15 were also employed. We chose the 10 mol % APTS co-condensed material because of its structural similarity to SBA-15 and also because of the suggested higher surface amine content of this material as compared to the other co-condensed materials studied. Furthermore, APTS-SBA-15 is comparable to the materials used previously as substrates for dendrimer functionalization.[30,31]

The nitrogen sorption isotherms before and after PEI functionalization are shown in Figures 2−4, 7, and 8. In all

Table 2. Amino Group Content in Different Materials[a]

material	wt% NH_2	n/w (mmol g^{-1})	Γ_{NH_2},tot (μmol m^{-2})	n_{acc}/w (mmol g^{-1})	Γ_{NH_2},acc (μmol m^{-2})	IEP
Co-condensed amino-silane						
CC10%-SBA-15	7.5	1.30		0.32	0.43	7.9
CC15%-SBA-15	6.1	1.04		0.28	0.42	8.5
CC20%-SBA-15	*11*	*1.90*		*0.20*	*0.31*	*8.7*
Aminosilanized samples						
APS-SBA-15	7.3			0.93	1.89	7.1
APTS-SBA-15	7			0.95	1.95	7.8
APDMES-SBA-15	6.9			0.90	1.50	8.0
APTS-SBA-15 RH	8.3			1.09	3.48	9
APTS-SBA-15 Ex	*10.3*			*1.19*	*2.69*	*7.9*
PEI-functionalized materials						
PEI-SBA-15	11	2.50	5.5		0.80	8.2
PEI-SBA-152^{cyc}	13.6	3.16	6.9		5.23	10.6
PEI-SBA-152^{cyc} TOT	23.2	5.39	18.0		5.23	10.6
PEI-SBA-15 RH	20	4.64	16.5		4.13	10.1
PEI-SBA-15 Ex	28	6.50	16.7		5.21	10.6
PEI-CC10%-SBA-15	20	4.67	26.5		6.16	10.6
PEI-APTS-SBA-15	7.5	1.74	5.5		4.33	10.3

[a] Total amount determined from TGA with respect to a reference sample; accessible amount determined by imine method and IEP from zeta-potential titrations.

cases, the PEI-functionalized SBA-15 substrates display a clearly lower specific surface area and pore volume, implying a successful incorporation of the polymer. The nitrogen sorption isotherms also reveal that no partial pore blocking has occurred upon functionalization, as the adsorption and desorption branches are almost parallel and exhibit a narrow hysteresis. Importantly, the lowering of the mesopore volume is much greater than what would be expected only from the increase in total mass due to the mass of the formed polymer, which indicates that the polymer is also situated inside the mesopore walls and certainly not only on the external particle surface. For the purely siliceous substrates, the microporosity is absent after PEI functionalization, indicating that the micropores have been filled by PEI. The mesopore diameters decrease slightly after PEI functionalization for the SBA-15 RH and SBA-15 Ex substrates, while the mesopore diameter remains virtually unchanged after PEI functionalization for the calcined SBA-15, which is in agreement with the much higher level of microporosity of the calcined SBA-15 support and thus with a larger fraction of PEI being present in the micropores in this case. A similar trend is observed in the *C*-values, as the PEI-SBA-15 RH and PEI-SBA-15 Ex materials have *C*-values less than 40, while the corresponding value for PEI-SBA-15 was 63. However, if a second round of aziridine polymerization was carried out, the mesopore diameter of PEI-SBA-15 also decreased, and the *C*-value decreased to the same level as that of the PEI-SBA-15 RH and PEI-SBA-15 extracted materials, indicating an increased level of amine functions present in the mesopores.

Also, for the co-condensed CC10% and the post-grafted APTS-SBA-15 substrates, a clear reduction in the specific surface areas, mesopore volumes, and *C*-values were observed upon PEI functionalization, with *C*-values in the range of 35−40. This was especially pronounced for the co-condensed substrate, where the pore volume decreased by about 68% and the specific surface area by 75%.

Amount of Amino Groups. The amount of amino groups in the different functionalized materials was determined both thermogravimetrically as well as by the imine method, which is based on selective condensation. The thermogravimetric method should be sensitive to the total amount of organic functions, while the imine method should be sensitive to the number of accessible (primary) amino groups. The results are presented in Table 2.

For the co-condensed materials, the total amount of incorporated amine varied between about 6 and 11 wt %. The value for the amino content in the materials obtained for the CC10%-SBA-15 material is the same as that reported in the original paper by Wang et al.,[17] while the values for the CC15%-SBA-15 and CC20%-SBA-15 materials are slightly lower. One reason for the observed differences could be that in our analysis, we referenced the obtained mass loss to that obtained for a corresponding material synthesized using only TEOS as the source for silica to account for mass loss related to the silica portion of the materials, as these materials are not calcined. While the CC20% material exhibits the highest weight loss of the studied co-condensed material, the imine reaction results suggest that this material has the lowest amount of accessible primary amines of the studied co-condensed materials, which is consistent with the *C*-value analysis based on the N_2 sorption data. It has been claimed that in the co-condensation process, the aminopropyl function is mainly incorporated via three oxygen bridges,[33] and thus, the observed weight loss can be directly related to the molar amount of amino functions in the material. Under this assumption, the fraction of accessible against incorporated functions can be calculated, and the results are given in Table 2. For the CC10% and CC15% materials, about 25% of the amine functions was detected by the imine method, while only 11% of the total amount of amino groups was detected for the CC20% material. This analysis suggests that most of the amino groups are embedded in the silica network (i.e., in the pore walls) and not located on the surface of the pores. Interestingly, the surface concentration of accessible amine groups is actually lower for the CC20%-SBA-15 material as compared to the CC10%-SBA-15 and CC15%-SBA-15 materials, which highlights the strong limitations connected to using data obtained by bulk analysis methods for estimating the surface concentration of introduced functional groups. The surface concentrations of amine

groups in the co-condensed materials, 0.3−0.4 μmol/m^2, can be compared with about 0.85 μmol/m^2 obtained for carboxylic acid-functionalized SBA-15 synthesized by co-condensation of TEOS and a cyano-silane with a silane content of 20 mol % in the synthesis.[15] The pronounced differences in the surface concentrations of functional groups can be understood, as the cyano-silane is much more hydrophobic than the amino silane under the employed acidic synthesis conditions, as the amine function will be protonated. Thus, while the cyano-silane can then act as a co-surfactant and be solubilized by the Pluronics micelles, and thus be located at the micelle−silica interface already during the synthesis, the driving force for solubilization of the much more hydrophilic protonated amino-silane will be much lower, leading to a much lower control of the location of the amino-silane during synthesis.

For the post-grafted materials, about 7 wt % amino functions was present in the functionalized calcined SBA-15 material, irrespective of the amino-silane used, although APDEMS has been shown to produce monolayers of the highest primary amine density on the surface of fused silica and oxidized silicon wafers as compared to a range of amino-silanes.[47] This value coincides with values reported in other studies on APTS-functionalized SBA-15 determined by TGA.[30,31] For the APTS-functionalized RH SBA-15, the corresponding value was 8 wt %, while as much as 11 wt % was obtained for the APTS-functionalized extracted SBA-15 substrate. Thus, our results follow the order of expected differences in the surface silanol concentration between the substrates. Note that only the weight percent of organics is given since the molar amount of amine cannot be directly determined thermogravimetrically for the post-grafted materials. This is due to uncertainty about the degree of hydrolysis and the exact means of surface binding of the amino-silane. It has even been proposed that the initial step of amino-silane adsorption to a silica surface is through hydrogen bonding between the amino group and the surface silanols[58,59] and that after adsorption the amine group can catalyze the condensation of the silicon side of the molecule with a surface silanol.[59] The amino group has been reported to relinquish its interaction with the silica during thermal curing, and the amino-silane molecule turns from an amine down position to an amine up position; also called the flip mechanism.[59] Without this curing step, APS is adsorbed mainly with its amine group onto the silanol groups of the silica surface.[60] Curing times of 3 h at 353 K have proven to be sufficient to achieve maximum silane−surface stability,[61] whereas the presence of surface water combined with curing temperatures greater than 423 K has been reported to optimize the number of siloxane bonds at the interface.[62] The influence of physisorbed water has been particularly stressed in surface modification of silica surfaces with APTS.[59,62,63] Some studies suggest that surface water is crucial for the silanization reaction,[62,64] while other reports state that the silanization reaction with APTS is self-catalyzed and that siloxane bonds formed also in the absence of water.[65] Maciel and co-workers found that whereas some surface water is desirable for optimizing the silylation process of APTS, too much water will interfere[62] since the highest silane loading level was achieved with silica gel dried at 25 °C and 10^{-2} Torr as opposed to drying at 473 K and 10^{-2} Torr, which should suffice to remove all water from essentially nonporous silica gel surfaces. Therefore, the drying conditions employed in the present study should be adequate to remove most of the excess water, while some physisorbed water will remain on the pore surface.

Silylation in dry toluene at 25 °C has been reported to provide a high silane loading,[62] but we did not find any remarkable differences in silane loading between samples functionalized at 298 K or under heat treatment. On the basis of the imine reaction results, it is clear that the amount of accessible amine functions is far higher for the post-grafted materials as compared to the co-condensed materials and that the surface excess of amine functions follows the order of the total content of amino functions, as can be expected, but also follows the order of decreasing degree of microporosity of the substrates. However, we note that the surface excess for the RH substrate if calculated based on unit area and not based on mass is higher than for the extracted material. Furthermore, it is interesting to note that the concentration of accessible amino functions is roughly the same as the amount of accessible silanols determined by benzylamine adsorption. However, this does not mean that there are no remaining silanols on the surface, as not all silanols are available for silanization reactions,[4,57,62] and uncondensed silanol groups belonging to the introduced silanes during post-functionalization could also be a source for residual silanols.

For the PEI-functionalized materials, the molecular weight for the function is approximately known, 42−44 g/mol depending on the degree of substitution on the nitrogen atom, and hence, the molar total concentration of amino groups can be estimated based on the weight loss in TGA. Fairly dramatic differences were observed for the different siliceous SBA-15 substrate materials, with weight percentages of PEI ranging from 11 to 28 wt % (see Table 2). Again, the amount of amino functions introduced increased in the order of calcined SBA-15 ≪ RH SBA-15 < extracted SBA-15 (i.e., the expected order for increased surface silanol concentration). This can be expected, as the surface hydroxyls are thought to serve as the sites from which the hyperbranched polymer is grown, being able to initiate the ring-opening polymerization of aziridine.[8] The relative amounts of accessible amino functions determined by the imine method follow

(58) Piers, A. S.; Rochester, C. H. *J. Colloid Interface Sci.* **1995**, *174*, 97.
(59) Vrancken, K. C.; Possemiers, K.; van der Voort, P.; Vansant, E. F. *Colloids Surf., A* **1995**, *98*, 235.
(60) Eklund, T.; Britcher, L.; Bäckman, J.; Idman, P.; Jokinen, A. E. E.; Rosenholm, J. B. In *Silanes and Other Adhesion Promoters*; Mittal, K. L., Ed.; VSP: Utrecht, The Netherlands, 2000; Vol. 2, p 55.
(61) Waddell, T. G.; Leyden, D. E.; DeBello, M. T. *J. Am. Chem. Soc.* **1981**, *103*, 5303.
(62) Caravajal, G. S.; Leyden, D. E.; Quinting, G. R.; Maciel, G. E. *Anal. Chem.* **1988**, *60*, 1776.
(63) Trens, P.; Denoyel, R. *Langmuir* **1996**, *12*, 2781.
(64) Simon, A.; Cohen-Bouhacina, T.; Porté, M. C.; Aimé, J. P.; Baquey, C. *J. Colloid Interface Sci.* **2002**, *251*, 278.
(65) (a) Vrancken, K. C.; van der Voort, P.; Vansant, E. F.; Grobet, P. *J. Chem. Soc., Faraday Trans.* **1992**, *88*, 3197. (b) Kallury, K. M. R.; MacDonald, P. M.; Thompson, M. *Langmuir* **1994**, *10*, 492.

the same order, and the surface excess per unit area for the RH substrate is about 5 times and that of the extracted substrate is about 6.5 times higher than that of the calcined SBA-15 substrate. These results are in good agreement with the N_2 sorption analysis, (micropore volume and *C*-value), which indicated that during the first polymerization cycle, micropores are preferentially filled by PEI for the calcined SBA-15 substrate, which naturally should lead to a lower surface excess of accessible amine groups. However, if a second cycle of PEI functionalization was performed for the calcined SBA-15 substrate, a total of 23 wt % PEI could be introduced, which rendered comparable surface excess values as for the extracted SBA-15 substrate after one PEI polymerization cycle. The PEI-functionalized materials showed typically 12 times higher surface excess values as compared to those obtained for the co-condensed materials and 2−3 times higher surface excess values as compared to those obtained for the post-grafted materials.

Finally, we return to the PEI-functionalized CC10%-SBA-15 and APTS-SBA-15 materials. The post-grafted substrate, APTS-SBA-15, actually exhibits the lowest amount of PEI incorporated of all studied substrates, 7.5 wt %, although here the total organic content is 13.7 wt %, taking the already present amino functions into account. This can be explained partly by the fact that a fair amount of the surface silanols has already reacted with the amino-silane. As for the co-condensed CC10%-SBA-15 substrate, even though the wt % aminopropyl is approximately the same and the effective amino concentration a fourth of the post-grafted concentration, the amount incorporated PEI is as high as 20 wt %. This may be explained by a combination of the significantly higher concentration of surface silanol groups for this solvent-extracted sample. In a study by Kim et al. related to PEI-functionalization of amino-silanized silica surfaces, starting from a density of primary amines of 3.5/nm^2 did not result in significant improvement of the final surface density of amino groups as compared to a starting density of 1.5/nm^2.[66] The explanation for this was that the final surface density was mainly controlled by the molecular volume that was governed by the van der Waals radii. Furthermore, it was noted that the growth accompanying the branching in solution usually stops after 3 or 4 generations due to steric encumbrance.[67] This fact has major implications on the growth of the polymer in a confined environment as a mesopore, and the growth of several generations in the mesopores cannot be expected. It should be kept in mind, however, that the spatially restricted environment such as the mesopore also involves limitations for the measurable maximal surface density of amines by the imine method, as was already recognized for flat surfaces.[47] However, as the materials under study are very similar, the values obtained for the accessible amount of amino groups are thought to be directly comparable. Furthermore, in many foreseen applications for this class of materials, such as drug release, immobilization of biomolecules, and other host−guest applications, guest molecules very similar in size to 4-nitrobenzaldehyde are typically used, and the values derived by the 4-nitrobenzaldehyde method may thus quite closely reflect the real surface concentration of accessible amino groups in such applications.

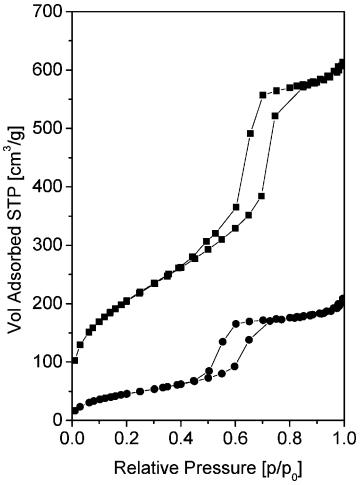

Figure 8. Nitrogen sorption isotherms measured at 77 K for CC10%-SBA-15 (■) and PEI-functionalized CC10%-SBA-15 (●).

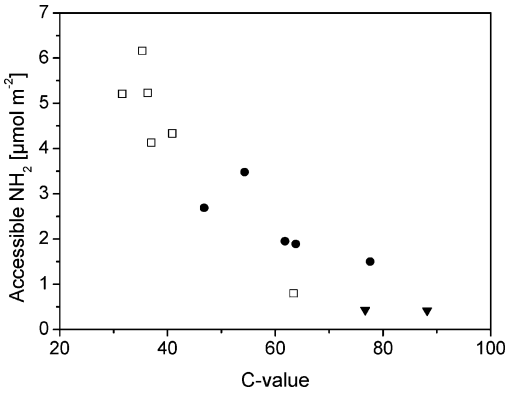

Figure 9. Accessible amount of amine groups for the functionalized materials as plotted against the *C*-value. Co-condensed materials (▼), post-grafted aminosilanized materials (●), and PEI-functionalized materials (□). Sample details can be found in Table 2.

The *C*-values and the surface concentrations of accessible primary amine groups determined by the imine method are plotted in Figure 9. The *C*-values derived for the microporous materials (i.e., the CC20%-SBA-15 and the SBA-15 substrate materials) have not been included in the analysis. A good correlation is observed, where the *C*-values increase with decreasing surface amine concentrations. This is to be expected, as the surface polarity decreases with an increasing surface concentration of organic amine groups. The *C*-values have previously also been correlated with the degree of surface functionalization of silica.[68,69] In a detailed study by Trens et al.,[69] related to the surface functionalization of macroporous silica by C_{18}-silanes, it was noted that the *C*-values indeed followed the degree of surface functionalization, but only up to a surface concentration of about 2 μmol/m^2. At higher surface concentrationss the *C*-value remained unchanged. This observation was related to the possibility of the aliphatic C_{18} chain laying flat on the silica

(66) Kim, H. J.; Moon, J. H.; Park, J. W. *J. Colloid Interface Sci.* **2000**, *227*, 247.
(67) Tomalia, D. A.; Naylor, A. M.; Goddard, W. A. *Angew. Chem., Int. Ed. Engl.* **1990**, *28*, 138.
(68) Jelinek, L.; Kováts, E. S. *Langmuir* **1994**, *10*, 4225.
(69) Trens, P.; Denoyel, R.; Glez, J. C. *Colloids Surf., A* **2004**, *245*, 93.

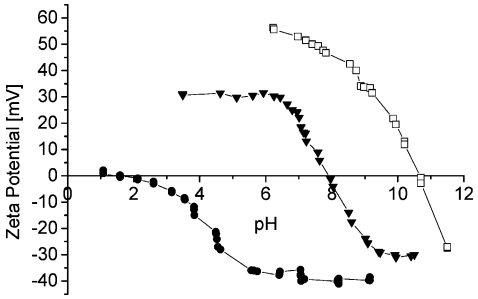

Figure 10. Zeta-potential titrations for SBA-15 (●), CC10%-SBA-15 (▼), and PEI-CC10%-SBA-15 (□). IEP values for all functinonalized materials are listed in Table 2.

surface, which made the surface hydrophobic already at fairly low surface concentrations. In our case, the surface function is much shorter, and we suggest that this is the main reason as to why the correlation between the *C*-value and the surface concentration is valid over a much wider surface concentration range in our case.

Zeta-Potential Titrations. Finally, we have characterized the materials electrokinetically by determining the isoelectric point, IEP, by measuring the zeta-potential as a function of pH. The zeta-potential is the potential at the slipping plane or the surface of the hydrodynamic shear in the electrical double layer surrounding charged particles. The titrations were performed in both directions (high and low pH) without any apparent hysteresis, suggesting that ionic strength differences or specific adsorption of introduced ions during the measurements performed without the addition of background electrolyte did not contribute to the results. The reversibility of the titration curves also indicates a good pH stability of the function. The zeta-potential measurements are sensitive to the surface potential measured just outside the particle surface and are not sensitive to the surface potential inside the porous particles. Amorphous silica has an IEP in the range of 2−3[70] and is controlled by the deprotonization of single or isolated (Q^3) silanol groups.[15] The presence of the amine function should shift the IEP toward higher pH values, as the pK_a of aminopropyl is 9.8 and PEI is 10.6, and the amine groups should be fully protonated at pH values of less than about 9. The IEP values determined for the different materials are given in Table 2, and selected zeta-potential titration curves are shown in Figure 10. For the purely siliceous SBA-15 materials, the IEP values were close to 2−3 as expected for amorphous silica. For the co-condensed materials, the IEP values were in the range of 7.9−8.7, where the IEP values increased with increasing APTS content in the synthesis. The increase in the IEP value as compared to that of pure silica is direct evidence for the presence of amino groups on the particle surfaces. The decreasing zeta-potential at pH values exceeding 7 is a consequence of two surface chemical events, the deprotonation of surface silanols generating negative surface charges and the deprotonization of positively charged R-NH_3^+ groups. We have recently shown[15] that the major fraction of the surface silanol groups of SBA-15 are ═Si-$(OH)_2$ (geminal) groups, which deprotonate with a pK_a value of about 8 for the first deprotonization step. Thus, an IEP

(70) Iler, R. K. *The Chemistry of Silica*; Wiley: New York, 1979.

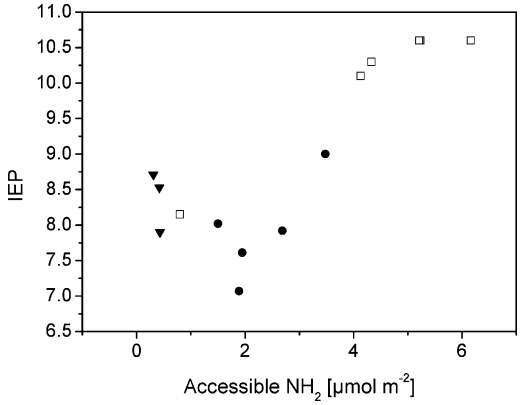

Figure 11. IEP plotted against the amount of accessible primary amine groups. Co-condensed materials (▼), post-grafted aminosilanized materials (●), and PEI-functionalized materials (□). Sample details can be found in Table 2.

value around 8 is a direct indication of the presence of free geminal (Q^2) silanols on the surface also on these amino-functionalized silica materials. In Figure 11, the IEP values are plotted against the surface amine concentrations determined by the imine method. Generally, a good correlation between the surface amine concentration and the IEP values is found for the post-grafted and PEI-functionalized materials, where an increase in the IEP value is observed with an increasing surface amine concentration, with a plateau in the IEP values around 10.6. For the co-condensed materials, the IEP values are clearly higher than the surface amine concentration would suggest. As the electrokinetic potential is sensitive to the surface charging of the outer particle surface, this suggests that the accessible amine groups are preferentially located on the outer particle surface for these materials. This is also true for the one cycle PEI-SBA-15 (calcined) material, where a major fraction of the PEI present inside the particle is located in the micropores of the silica substrate. However, the IEP for this material also exceeded 10 when the PEI functionalization was repeated a second time. The post-grafted materials all have IEP values in the range of 7−9, and the highest IEP value was obtained for the RH material for this group of materials. This was also the material that exhibited the highest surface excess of amino functions calculated per unit area for the post-grafted materials.

We note that the sole fact that all the materials, including the PEI-functionalized materials, exhibit an IEP suggests that in all cases some free surface silanols are still present on the particle surfaces, to an extent that is directly related to the IEP of the materials. We also note that the observed differences between the materials in terms of their electrokinetic mobility as a function of pH and the good correlation found between the zeta-potential results and the other used means for surface characterization are important for the use of amine-functionalized mesoporous silica in biological applications where the pH conditions most often are close to neutral. Depending on the effective surface concentration of the amine groups and the surface concentration of the free silanol groups, the electrokinetic surface potential could vary from slightly positive to strongly positive under these

conditions, due to the charge balancing effect of the deprotonating surface silanols.

Conclusion

Amino-functionalized mesoporous SBA-15 materials prepared by post-grafting, co-condensation and surface polymerization of a polyethylene-imine, respectively, have been studied by wet-chemical methods, with a special focus on the amount of accessible amino groups. The number of accessible primary amino groups was compared to the total amount of incorporated amino functions, allowing information to be obtained about the relative amount of functional groups embedded in the silica network or embedded in micropores of the substrate. The co-condensation route was the least efficient surface functionalization method under the studied conditions, while surface polymerization lead to the highest number of accessible amine groups. However, often, the first polymerization cycle lead to polymer formation in the micropores of micropore-containing substrates, which renders these amine groups inaccessible. Good agreement was observed between the *C*-values obtained from BET surface area analysis and the amount of accessible primary amino groups obtained by imine formation. Furthermore, zeta-potential measurements yielded indirect information about the relative amount of amino functions and silanol groups being present at the outer surface of the mesoporous silica particles. This effect seems to be most pronounced for co-condensed materials and could possibly be connected to the formation of smaller particles in this case, stabilized with a higher concentration of amino groups on their outer surface. It was also shown that bulk analysis methods are generally not applicable for the determination of the amount of accessible surface functions. The results are suggested to be of importance for allowing results obtained for amino-functionalized materials in different applications to be rationally explained and thus for reaching a higher level of understanding of structure−activity relationships for this interesting class of materials.

Acknowledgment. The National Biomaterials and Tissue Engineering Graduate School is gratefully acknowledged for financial support (J.M.R.). M. Sc. Antti Penninkangas is acknowledged for the synthesis of aziridine. Dr. Matthias Thommes and Prof. Renaud Denoyel are thanked for useful discussions concerning the nitrogen adsorption results.

CM071289N